




Cite this: *RSC Adv.*, 2022, 12, 13192

Controlled release of silibinin in GelMA hydrogels inhibits inflammation by inducing M2-type macrophage polarization and promotes vascularization *in vitro*†

Weijian Xu,^{‡a} Yingjia Sun,^{‡a} Jia Wang,^c Baixiang Wang,^b Fanxing Xu,^d Zhijian Xie ^{*a} and Yu Wang ^{*b}

A dry socket is one of the most common complications after tooth extraction. The main etiologies are the loss of blood clots in the socket and the inflammation reaction caused by infection. Current studies on how to prevent dry sockets could not solve these two etiologies at the same time. Recent studies have demonstrated the anti-inflammation role of silibinin. In this study, silibinin was engineered into GelMA hydrogels (Sil-GelMA) with a concentration of 30 mM. The surface characteristics were observed by scanning electron microscopy and the successful loading of silibinin was detected by FTIR spectrometry. The Sil-GelMA hydrogels presented the sustained release ability of silibinin and slow degradation performance of GelMA. Furthermore, silibinin inhibited the inflammatory reaction by inducing M2-type macrophage polarization, promoting the secretion of anti-inflammatory factors (CD206, IL-10) and inhibiting the secretion of anti-inflammatory factors (IL-1 β , iNOS). Silibinin also increased the secretion of vascularization-related factor VEGF and promoted vascularization *in vitro*. This study suggested that the Sil-GelMA hydrogels not only had an anti-inflammatory effect, but also had the potential to promote vascularization. Based on these results, the Sil-GelMA hydrogels might provide a promising prospect for prevention of dry sockets in the future.

Received 24th January 2022
Accepted 5th April 2022

DOI: 10.1039/d2ra00498d

rsc.li/rsc-advances

Introduction

A dry socket is one of the most common postoperative complications after tooth extraction, especially in the third molar, which is also known as alveolar osteitis, fibrinolytic alveolar osteitis, localized osteomyelitis, *etc.*¹ The main clinical feature is severe pain occurring 3–4 days after tooth extraction, which can radiate to the auriculotemporal, mandibular area or the top of the head, and the pain cannot be relieved by general analgesic

drugs. Meanwhile, dry socket is also accompanied by empty socket, bad breath, and other symptoms. The etiology of dry socket is still not clear, and may be related to infection, trauma, smoking, anatomy, and other factors.² The absence of the blood clot in the socket and the inflammation caused by infection are considered to be the main causes.³ The first day after tooth extraction, it is of great significance to maintain the stability of blood clots in the socket. It has the highest risk of infection within 3 days after tooth extraction. Currently, there is no fully effective way for prevention of dry sockets. Some potential solutions are proposed and being investigated by researchers including mouthwash used pre and post-extraction,⁴ application of antibiotics^{5,6} and use of absorbable collagen sponges.⁷ However, all of these approaches could not both protect the blood clots in the socket and inhibit inflammation caused by bacterial infection. Therefore, an effective method is needed to be explored to maintain the stability of blood clots in the socket and inhibit the inflammation at the same time.

Macrophages are one of the most important components of the innate immune system, and play roles in inflammation, defense, repair, metabolism, and other physiological processes.⁸ Macrophages can change phenotypes, which is known as polarization. M1-type (classically activated macrophages) are mainly involved in pro-inflammatory responses and

^aDepartment of Oral and Maxillofacial Surgery, Stomatology Hospital, School of Stomatology, Zhejiang University School of Medicine, Zhejiang Provincial Clinical Research Center for Oral Diseases, Key Laboratory of Oral Biomedical Research of Zhejiang Province, Cancer Center of Zhejiang University, Hangzhou 310006, China

^bDepartment of Oral Implantology, Stomatology Hospital, School of Stomatology, Zhejiang University School of Medicine, Zhejiang Provincial Clinical Research Center for Oral Diseases, Key Laboratory of Oral Biomedical Research of Zhejiang Province, Cancer Center of Zhejiang University, Hangzhou 310006, China. E-mail: wangyuzju@zju.edu.cn

^cStomatology Hospital, School of Stomatology, Zhejiang University School of Medicine, 166 Qiutaobei Road, Shangcheng District, Hangzhou, Zhejiang, 310016, China

^dWuyi College of Innovation, Shenyang Pharmaceutical University, Shenyang 110016, P. R. China

† Electronic supplementary information (ESI) available. See <https://doi.org/10.1039/d2ra00498d>

‡ These authors contributed equally.



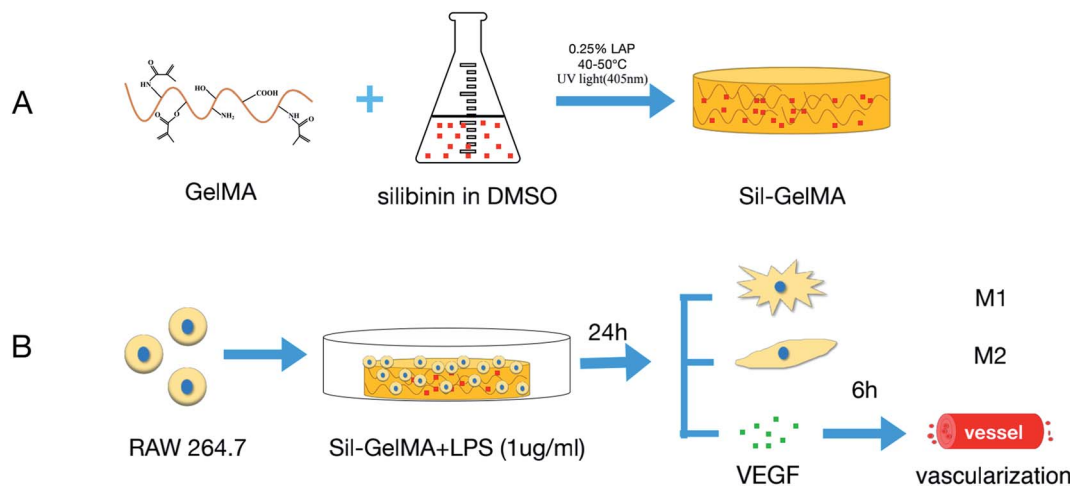


Fig. 1 Schematic illustration of the experiment design. (A) Preparation of Sil-GelMA hydrogels, (B) *in vitro* experiment process of this study.

M2-type (alternatively activated macrophages) are mainly involved in anti-inflammatory responses both M1-type and M2-type are closely related to inflammatory responses. Cytosines and microbial products profoundly and differentially affected the function of macrophages,⁹ which acted by promoting the orientation of adaptive responses in an M1-type or M2-type direction.^{10–13} For example, when pathogens invade the organism, macrophages are precisely polarized to M1-type, and alter the tissue micro-environment by producing a large number of inflammatory factors, then kill the invading pathogens and activate the adaptive immunity. In the meanwhile, these inflammatory factors also induce M2-type polarization, and then alleviate inflammation, avoid excessive injury, and promote wound healing.^{14,15} Therefore macrophage polarization is of great significance for controlling the early stage of inflammation. Infection is one of the main causes of dry socket, which causes local inflammation. Exploring and controlling macrophages polarization may provide a new treatment approach for preventing inflammation in dry socket.

Silibinin is a natural product which is composed of a blend of two diastereomers: silybin A and silybin B, mostly in equimolar proportions.¹⁶ It is the main component of milk thistle seeds extract. Previous studies have demonstrated the antioxidant and anti-inflammatory functions of silibinin.¹⁷ N. M. Vargas *et al.* found that silibinin inhibited inflammatory responses mainly through Nrf2 and NF- κ B signalling pathways.^{18,19} C. K. Youn *et al.* discovered that silibinin inhibited LPS-induced macrophages activation by blocking p38 MAPK in RAW 264.7 cells, which resulted in the inhibition of inflammatory factor expression (iNOS, TNF- α and IL-1 β).²⁰ Therefore, we speculated that if silibinin was placed into the socket after tooth extraction, it might be helpful for the early prevention of dry socket.

An optimized wound healing process depends on an adequate vascularization of the socket space.²¹ Blood clots contain high level of vascular endothelial growth factor (VEGF), and also provide space support for vascularization.²² One major problem with dry socket is the loss of blood clots in the socket, which leads to insufficient space and cytokines for

vascularization. To solve this problem, it is desirable to keep space stability in the socket. GelMA hydrogels, with a series of advantages, such as good biocompatibility (including biosafety and biological functionality), strong cell adhesion, controlled drug release performance and tunable physicochemical properties, were widely used in the field of tissue engineering.^{23,24} In this study, GelMA hydrogels were used as a carrier for silibinin. It was hypothesized in this research that the silibinin–GelMA (Sil-GelMA) hydrogels release system could keep spatial stability in 24 hours, and silibinin can be slowly released. The goal of this study is to determine whether the Sil-GelMA hydrogels can induce macrophages to polarize into M2-type, and promote the effect of anti-inflammation and vascularization *in vitro* (Fig. 1).

Experimental

Cell culture and seeding

Mouse monocyte-macrophage RAW 264.7 cells (ATCC; TIB-71, Cell Bank of Chinese Academy of Sciences, China) were cultured in Dulbecco's Modified Eagle Medium (DMEM; Gibco, Invitrogen Corp., USA) supplemented with 10% fetal bovine serum (FBS; GIBCO, Grand Island, NY, USA), 100 IU ml^{−1} penicillin and 100 mg ml^{−1} streptomycin at 37 °C in 5% CO₂. The media was refreshed every 2 days. Human umbilical vein endothelial cells (Huvecs; ATCC; CRL-1730) were cultured in Endothelial Cell Medium (ECM; ScienCell) supplemented with 10% fetal bovine serum, 100 IU ml^{−1} penicillin and 100 mg ml^{−1} streptomycin at 37 °C in 5% CO₂. The media was refreshed every 2 days.

Cell proliferation assay. To determine the proliferation rate and the optimal concentration of silibinin, different concentrations (0, 10, 20, 30, 40, 50 mM) of silibinin were placed into a 24-multiwell plate which contained 500 μ L cell suspension with a density of 5×10^4 RAW 264.7 cells per well. A cell counting kit-8 (CCK-8, Dojindo Laboratories, Japan) was used to measure the cell proliferation rate by a microplate reader at 450 nm. Then, the optimal concentration of silibinin was determined.



Preparation of silibinin–GelMA hydrogels release system

The GelMA hydrogels release system was prepared as reported previously.²⁴ Silibinin (R014957, RHAWN, Shanghai, China) was dissolved in DMSO (D2650, Sigma-Aldrich, St. Louis, MO, USA) at the concentration of 1 M for preservation. After being shaken well, 0.25% photoinitiator LAP (EFL, Suzhou, China) was dissolved in phosphate-buffered saline (PBS). The LAP solution was preheated in the water bath at 40–50 °C for 15 min. Then, GelMA (EFL-GM-30, Suzhou, China) was added into 0.25% photoinitiator LAP standard solution at 5% mass percentage and placed in a water bath at 40–50 °C for 30 min. Finally, a DMSO solution of silibinin was added into the GelMA-LAP solution to reach the final concentration at 30 mM. A 0.22 µm filter was used for filtration. The Sil-GelMA hydrogels release system was prepared by UV-irradiation at the wavelength of 405 nm for 30 s.

Analysis of Sil-GelMA hydrogels characteristics

Sil-GelMA hydrogels were freeze-dried at –50 °C for 24 hours. The morphology of the dried Sil-GelMA hydrogels was observed by scanning electron microscopy (SEM; SU8010FE-SEM, HITACHI, Tokyo, Japan). To analyze the structural differences between GelMA and Sil-GelMA, the porosity of the two groups were measured by image J 1.52a. To analyze the existence of silibinin and its interaction with GelMA, the dried Sil-GelMA hydrogels were mixed with KBr, and the samples were ground to a powder and compressed into a thin sheet (<10 µm). The structures of all groups (Sil-GelMA, GelMA and silibinin) were investigated by FTIR Spectrometer (FTIR; NicoLET iS50FT-IR, Thermo Scientific, America). The wavelength ranged from 400–4000 cm^{–1} and the resolution was 4 cm^{–1}.

Measurements of silibinin release in Sil-GelMA hydrogels

To measure the release effect of silibinin from Sil-GelMA hydrogels in different pH environments, the hydrogels were placed in PBS (pH = 5.6 and pH = 7.4 respectively) in an incubator at 37 °C. Several time points were set up: 0, 2, 4, 10, 24, 36, 48, 80, 96 hours. At each detected time point, the original PBS solution was exchanged by fresh PBS. The released silibinin was quantified using Ultra Performance Liquid Chromatography (UPLC; Agilent 1290, America) by measuring the absorption peak of the silibinin at a wavelength of 288 nm. A corresponding calibration curve was applied to confirm the concentration.

Encapsulation efficiency and drug loading capacity calculations

Sil-GelMA hydrogels ($n = 3$) were degraded overnight in 2 mL of 0.1 units per mL collagenase II (CAS NO.9001-12-1; Gibco) in PBS solution. The degradation was carried out at 37 °C. The amount of silibinin was quantified using Ultra Performance Liquid Chromatography by measuring the absorption peak of the silibinin at a wavelength of 288 nm. The encapsulation efficiency (EE) and the drug loading capacity (LC) of the Sil-GelMA hydrogels were calculated using eqn (1) and (2).

$$EE(\%) = \frac{W_s}{W_d} \times 100\% \quad (1)$$

$$LC(\%) = \frac{W_s}{W_s + W_g} \times 100\% \quad (2)$$

W_d was the total weight of silibinin added, W_s was the weight of loaded silibinin and W_g was the weight of GelMA hydrogels.

Degradation study

Type II collagenase (CAS NO.9001-12-1; Gibco) was added separately into GelMA hydrogels and Sil-GelMA hydrogels at the concentration of 1 U ml^{–1}.^{25,26} The samples were freeze-dried for 24 hours, and the initial weight (W_0) of all the samples was measured. Then the freeze-dried samples were kept in PBS in an incubator at 37 °C. The PBS was refreshed every 8 hours. The samples were then taken out and dried under vacuum at 50 °C at predetermined time intervals and final weight (W_t) was measured. The degradation rates were calculated using eqn (3).

$$\text{Degradation rate } (\%) = \frac{W_0 - W_t}{W_0} \times 100\% \quad (3)$$

In vitro cell morphology observation

RAW 264.7 cells cultured in different groups (silibinin, Sil-GelMA, GelMA and the control) were collected after 24 hours with the stimulation of LPS (1 µg ml^{–1}; Sigma-Aldrich, St. Louis, MO, USA). Cell morphologies were observed by optical microscope.

Flow cytometry analysis

RAW 264.7 cells cultured in different groups (Silibinin, Sil-GelMA, GelMA and the control) were collected after 24 hours with the stimulation of LPS. The density of cell suspension prepared was 1×10^6 per ml. CD206 (#MA5-16871) and CD86 (#11-0862-81) were used for flow cytometry (CytoFLEX LX, America).^{27,28}

Gene expression analysis

RAW 264.7 cells with the cell density of 5×10^4 cells per well were cultured in different groups (silibinin, Sil-GelMA, GelMA and the control) with the stimulation by LPS (1 µg ml^{–1}) at the same time. After 24 hours, cells were collected and total RNA from different groups were extracted using the TRIzol kit (Invitrogen, Carlsbad, CA, USA) according to the protocol, following DNaseI treatment and reserve transcription.²⁹ To analyze the expressions of CD206, IL-10, IL-1β, iNOS, and VEGF, real-time PCR was performed with SYBR green by the 2^{–ΔΔCT} method. The primers for the target genes are listed in Table 1.

Tube formation assay

RAW 264.7 cells were cultured in different groups (silibinin, Sil-GelMA, GelMA and the control) with the density of 5×10^4 cells per well, and were stimulated by LPS (1 µg ml^{–1}) at the same time. After 24 hours, the supernatant culture mediums of



Table 1 The primers for the target genes used in real-time PCR

Gene	Primer sequences (5'–3')
IL-10	F: TTCTTTCAAACAAAGGACCAGC R: GCAACCCAAGTAACCCCTTAAAG
VEGF α	F: TAGAGTACATCTTCAAGCCGTC R: CTTTCTTTGGTCTGCATTACACA
CD206	F: CCTATGAAAATTGGGCTTACGG R: CTGACAAATCCAGTTGTTGAGG

different groups were collected. Huvecs were cultured for 6 hours in supernatant culture mediums from different groups mentioned above. Then, tube formation phenomenon was observed by optical microscope.

Statistical analysis

In vitro experiments were carried out three times to obtain mean and standard error from independent experiments. ANOVA (analysis of variance) and Student's *t*-test were performed to determine the significant differences between the groups. *P* < 0.05 was considered statistically significant.

Results and discussion

Cell proliferation assay and drug concentration test

In this study, cell proliferation assay was first performed to test the effect of silibinin on RAW 264.7 cell proliferation and the optimal drug concentration was determined. The results showed that DMSO, as a solvent of silibinin, had no significant effect on RAW 264.7 cell proliferation compared to the control group (0 mM + DMSO(–) group). These two groups demonstrated the good cell viability of RAW 264.7 cells in normal condition. Meanwhile, with the concentration less than 30 mM, silibinin showed no inhibition on RAW 264.7 cell proliferation compared to the control group (0 mM + DMSO(–) group). It was reported that the anti-inflammatory effect of silibinin is positively correlated with a concentration when it is less than 50 mM.¹⁹ These results showed that silibinin had good biocompatibility and no inhibition on RAW 264.7 cell proliferation was observed with the concentration less than 30 mM. Therefore, 30 mM was chosen as the optimal concentration for the next research (Fig. 2).

Characteristics of Sil-GelMA hydrogels

SEM was used to study the microstructure of the Sil-GelMA hydrogels, and the results were shown in Fig. 3. The SEM showed that GelMA hydrogels had a 3D microporous structure and the internal structure was not damaged by the addition of silibinin (Fig. 3B). The average pore size of GelMA hydrogels was $50 \pm 8.7 \mu\text{m}$, as shown in the cross-sectional image (Fig. 3A). It has been reported that different types of cells could adhere to and grow on the surface of GelMA substrates, and cells can be encapsulated within the GelMA hydrogel matrixes with excellent viabilities.^{30,31} In Fig. 4B, a layer of sediment was found on the surface of the Sil-GelMA hydrogels, which was possibly the

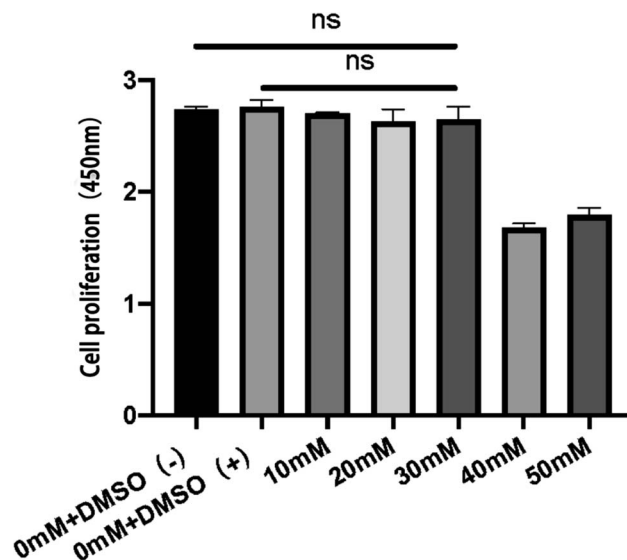


Fig. 2 Effects of different concentrations of silibinin on proliferation of RAW 264.7 cells. RAW 264.7 cells were cultured in DMEM with different concentrations of silibinin (0, 10, 20, 30, 40, 50 mM). Cells were harvested 24 hours later. The proliferation test was carried out using CCK-8. "ns" represented no significant difference (*p* > 0.05).

undissolved silibinin. The porosity of the Sil-GelMA group ($38.31\% \pm 2.70\%$) was lower than that of the GelMA group ($46.20\% \pm 6.24\%$) (*p* < 0.05) (Fig. 5). Silibinin loading reduced the porosity of GelMA hydrogels, which increased the hydrogel surface contact area with silibinin and cells.

GelMA is made from methacrylic anhydride (MA) and gelatin,²³ which contains the N–H structure. Silibinin contains the benzene ring and aromatic ether (Ar–O–R), which is the peculiar structure in silibinin (Fig. 6A). FTIR analysis were performed to identify the structures of silibinin, GelMA and Sil-GelMA hydrogels. As shown in Fig. 6B, an absorption peak could be observed in both silibinin and Sil-GelMA groups at the wavelength near 1500 cm^{-1} , which was attributed to the skeleton vibration of the benzene ring. Also, the absorption band of silibinin showed peaks in 950 cm^{-1} and 1230 cm^{-1} , which corresponded to R–O and Ar–O respectively. These characteristic absorption peaks could be found in Sil-GelMA hydrogels as well. The absorption band of GelMA showed a peak occurred at 1640 cm^{-1} corresponds to N–H stretching (characteristic absorption of GelMA), which also expressed in Sil-GelMA hydrogels. These findings indicated that silibinin had been successfully assembled into GelMA without structure damage in both silibinin and GelMA during the assembly process.

The release kinetics of silibinin in different pH environments was further studied in this research. There are two release stages: burst release and sustained release.³² In both two pH environments, silibinin was quickly released on the first day, then stayed at a relatively slow and stable rate after then. Three days later, the release rate reached to a stable level. Silibinin released faster in environment with pH = 7.4 than that with pH = 5.6 within 36 hours, then the release rate became faster in environment with pH = 5.6 than that in environment



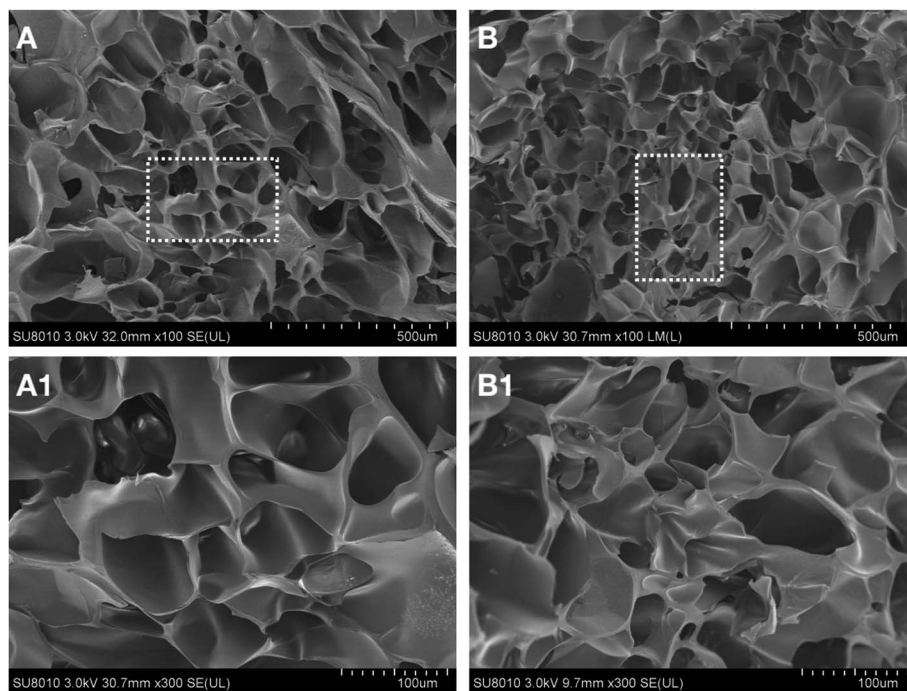


Fig. 3 Morphological characteristics of different groups at room temperature. (A) The GelMA group, (B) The Sil-GelMA group. A-1 and B-1 were the square parts of A and B respectively.

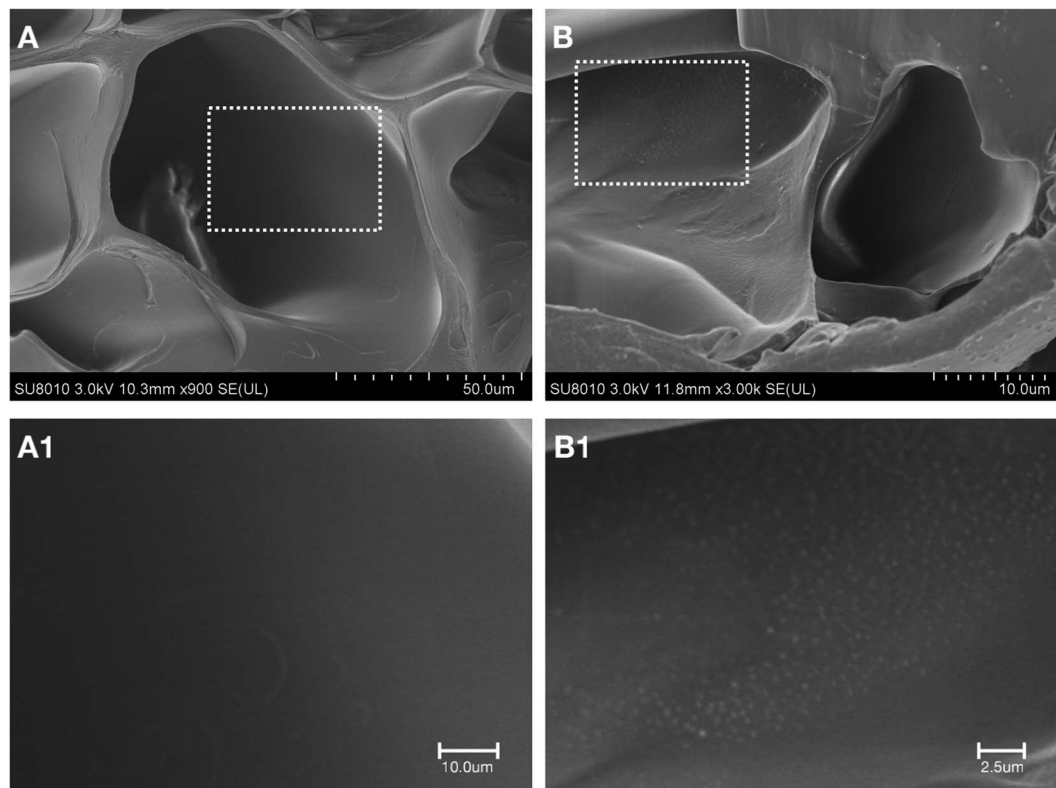


Fig. 4 Amplifications of the GelMA group and the Sil-GelMA group at room temperature. (A) The GelMA group, (B) The Sil-GelMA group. A-1 and B-1 were the square parts of A and B respectively.



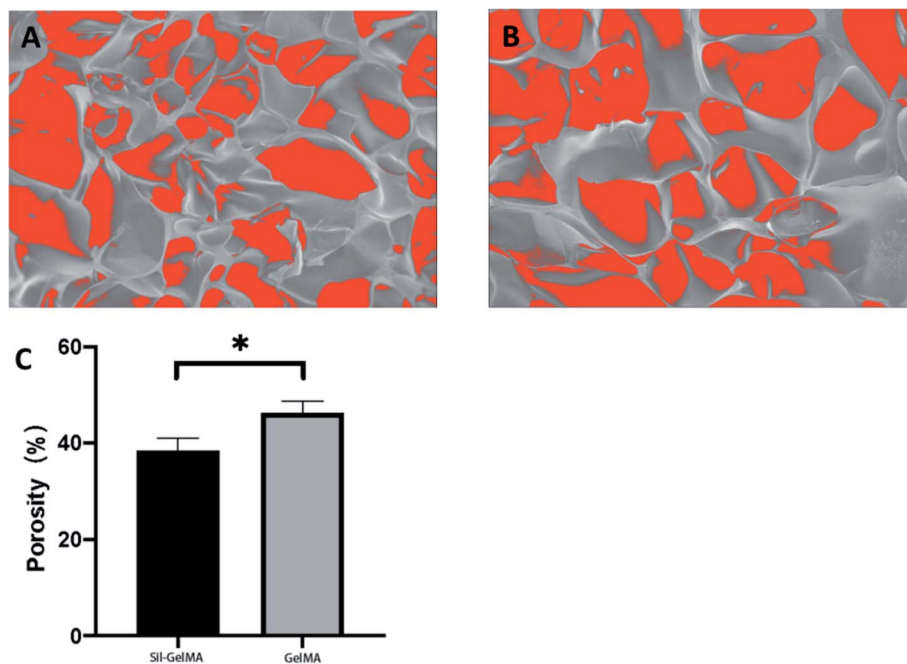


Fig. 5 Porosity of different groups. (A) The Sil-GelMA group, (B) the GelMA group, (C) quantification of the porosity of two groups ($p < 0.05$).

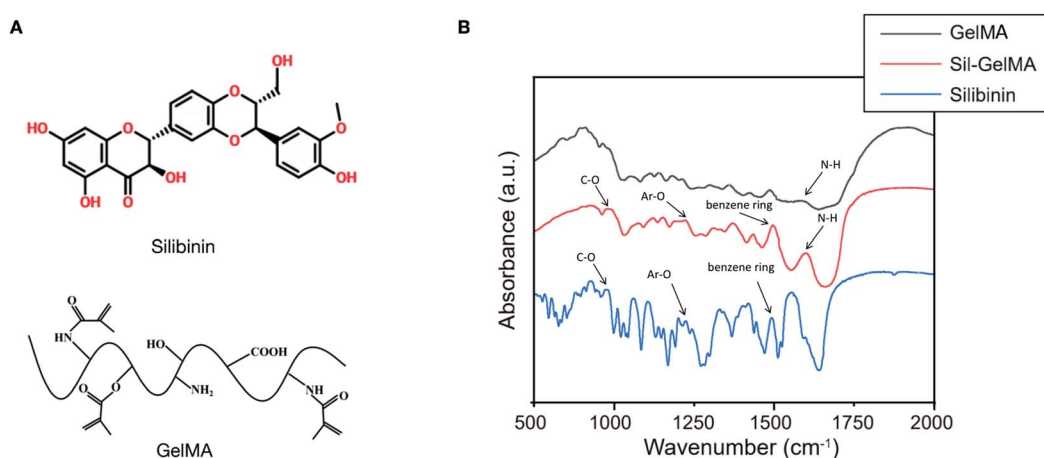


Fig. 6 (A) The structure illustration of silibinin and GelMA. (B) Chemical element analysis of different groups by FTIR.

with pH = 7.4. This suggested that silibinin might play a major role at the early stage and the Sil-GelMA hydrogels could also play a slow-release role in acidic environments (Fig. 7). The study then calculated the EE and LC of Sil-GelMA according to the equations mentioned above. The EE of Sil-GelMA was $88.2\% \pm 3.5\%$ and the LC was $19.05\% \pm 2.72\%$. These results indicated that GelMA hydrogels provided a favorable environment for silibinin loading.³³

Studies had proved that GelMA hydrogels could be applied as scaffolds for 3D cell culture by providing a mechanical tenable environment for cells and supporting cell adhesion, growth, and proliferation.^{34–37} As shown in the study, Sil-GelMA degraded by 43% within 24 hours, and the remaining hydrogels maintained the stability of the space, which could support

RAW 264.7 cells to adhere, grow, and proliferate. There was no significant difference in the degradation rate between GelMA and Sil-GelMA groups, both of which were completely degraded in 3 days (Fig. 8). Based on these results, it suggested that Sil-GelMA hydrogels sustained a steady concentration of silibinin and could help to maintain the space stability during the early 24 hours.

Sil-GelMA hydrogels inhibit inflammation at an early stage *in vitro*

Macrophages stimulated with LPS mainly polarize into M1-type, which secrete pro-inflammatory factors and exert a strong cytotoxic and anti-proliferative effect.³⁸ On the other hand, IL-4/IL-13 stimulates the polarization of M2-type macrophages,



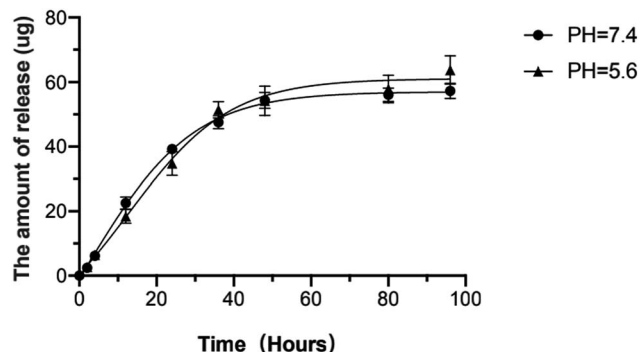


Fig. 7 *In vitro* release of silibinin from GelMA in different pH environments at 37 °C (pH = 7.4 and pH = 5.6). The curve represented the amount of released silibinin at different time intervals (0, 2, 4, 10, 24, 36, 48, 80, 96 h). Mean \pm SD, $n = 3$.

which contribute to inflammation resolution by secreting anti-inflammation factors and promoting wound healing.^{38,39}

The morphology results showed that after stimulated by LPS for 24 hours, RAW 264.7 cells exhibited two different polarization types. As shown in Fig. 9, in the silibinin and Sil-GelMA groups, a number of cells were fusiform with fewer synapses on the surface, few cells were radiated (Fig. 9A and B). However, in the GelMA and control groups, there was an enlargement in cell size, and the surface synapses increased and adhered tightly on the surface of the culture dish (Fig. 9C and D). Studies had proved that M1-type macrophages mainly presented as radiated shape, while M2-type macrophages mainly presented as fusiform shape.¹³

To better understand the effect of silibinin on macrophage polarization, this study detected the levels of macrophages-related markers, including CD86 for M1-type and CD206 for M2-type.^{40,41} As showed in Fig. 10, flow cytometry assay revealed that expression of CD206 was upregulated in macrophages of silibinin (71.88%) and Sil-GelMA (68.24%) groups compared to cells in GelMA (44.37%) and control (27.35%) groups ($p < 0.05$). There was no obvious difference between the silibinin group

and the Sil-GelMA group. It suggested that silibinin induced the polarization of macrophages towards M2-type, which conformed to the morphology experiment and the previous research mentioned above the expression of CD206 in macrophages in the GelMA group was higher than that in the control groups ($p < 0.05$). It was suspected that GelMA improved macrophage aggregation and induced a series of macrophage activation and polarization in order to enhance the role of anti-inflammation.⁴² Meanwhile, the expression of CD86 was down-regulated in macrophages of the silibinin (29.04%) and Sil-GelMA (27.41%) groups compared to macrophages in GelMA (45.98%) and control groups (49.02%) ($p < 0.05$). There was no obvious difference between the silibinin group and the Sil-GelMA group on CD86 expression. Macrophages were mainly induced into M1-type after stimulated by LPS.³⁸ However our results proved that silibinin inhibited the polarization of M1-type and promoted the polarization of macrophages to M2-type, which acted the anti-inflammatory effect when cells were stimulated with LPS.

To investigate the function of silibinin on inflammation, several target genes were further examined at the mRNA level such as CD206, IL-10, IL-1 β , iNOS. The mRNA expression of IL-10 was significantly higher in macrophages of the silibinin and Sil-GelMA groups than that of the GelMA and control groups at the time point of 12 hours and 24 hours ($p < 0.05$). IL-10 was a cytokine with a central role in inhibiting infection by limiting the immune response to pathogens and thereby preventing damage to the host.⁴³ This meant that silibinin had the effect on promoting the secretion of anti-inflammatory factors. Moreover, the mRNA expression of IL-10 was higher in the silibinin group than that of the Sil-GelMA group at the early stage (6 hours and 12 hours) ($p < 0.05$), which showed no difference at the time point of 24 hours (Fig. 11A). This might because the silibinin concentration in the silibinin group was higher than that in the Sil-GelMA group at the early stage. The mRNA expression of CD206 in macrophages was significantly higher in the silibinin and Sil-GelMA groups than that of the GelMA and control groups ($p < 0.05$), and it was higher in the silibinin

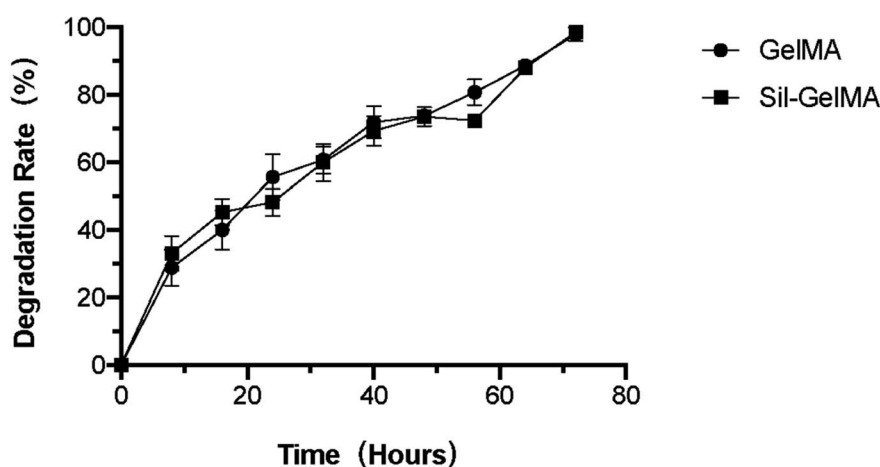


Fig. 8 Degradation rate of different groups under the action of type II collagenase at the concentration of 1 U ml⁻¹.



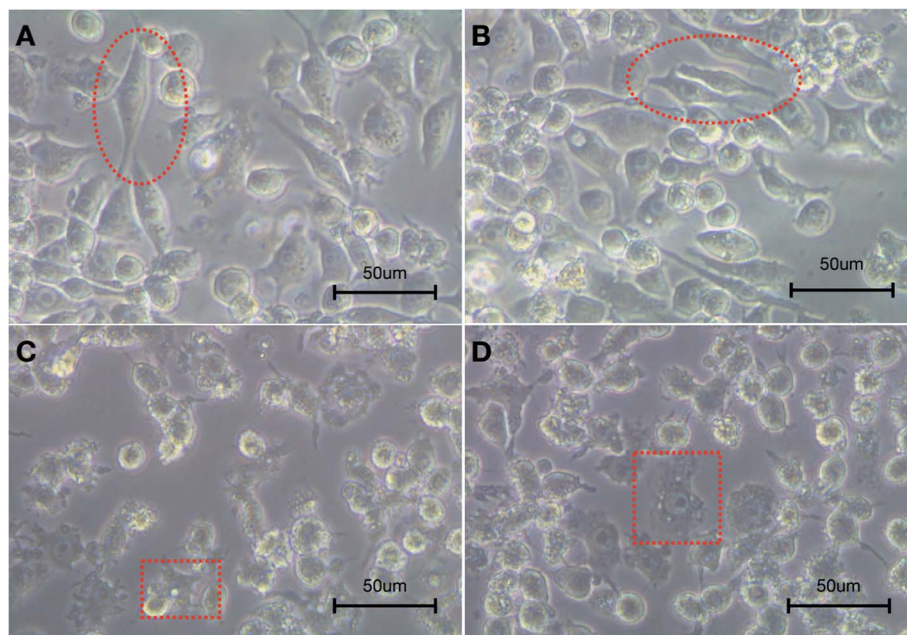


Fig. 9 Cell morphology of macrophages. RAW 264.7 cells cultured in different groups (silibinin, Sil-GelMA, GelMA and the control) were collected after 24 hours with the stimulation of LPS. The cell morphology was observed by optical microscope. (A) The silibinin group, (B) the Sil-GelMA group, (C) the GelMA group, (D) the control group. Circles indicated M2-type macrophages. Squares indicated M1-type macrophages.

group than that of the Sil-GelMA group within 24 hours (Fig. 11B). The stimulation of LPS provided an inflammatory micro-environment for macrophages, and the mRNA expression level of IL-10 and CD206 were down-regulated in the GelMA and control groups. With the slow release of silibinin from Sil-GelMA hydrogels, the mRNA expression of anti-inflammatory

factors in macrophages increased significantly in the silibinin and Sil-GelMA groups, which were secreted by M2-type macrophages. This suggested that the addition of silibinin promoted the polarization of macrophages towards M2-type.

The mRNA expressions of IL-1 β and iNOS showed a similar trend, which were significantly lower in macrophages in the

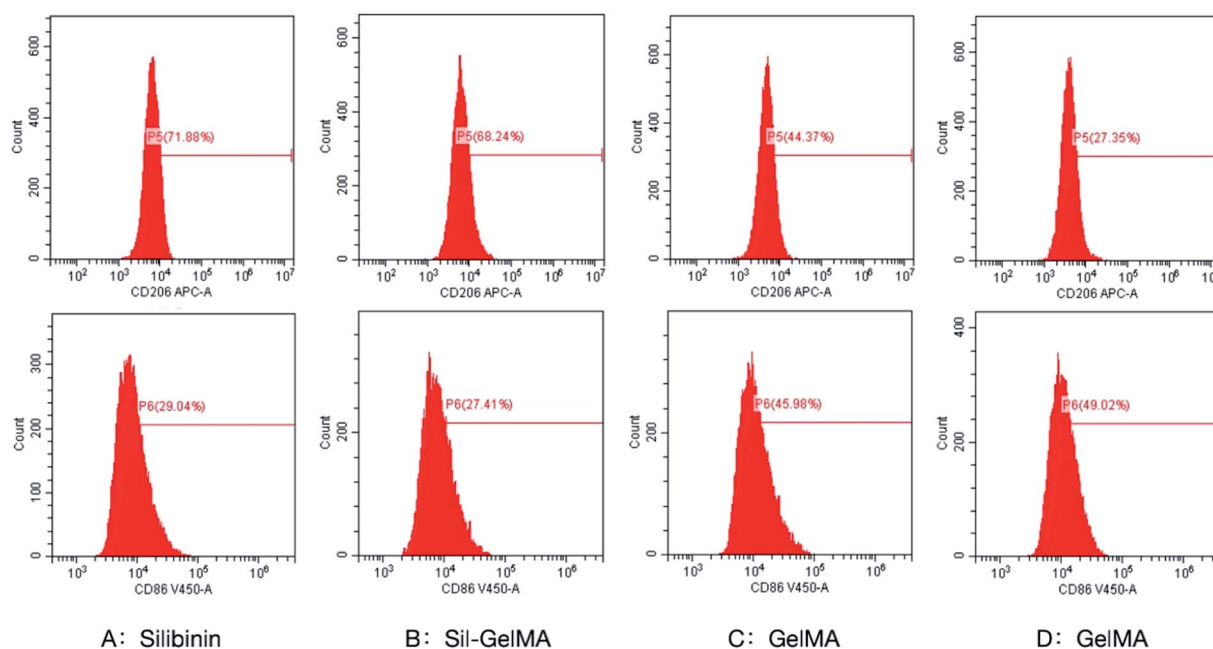


Fig. 10 Effect of silibinin on polarization of macrophages. Surface-specific markers of M1 and M2 macrophages were tested by flow cytometry analysis after 24 hours culture in different groups. The markers were CD86 (M1-type) and CD206 (M2-type). (A) The silibinin group, (B) the Sil-GelMA group, (C) the GelMA group, (D) the control group.

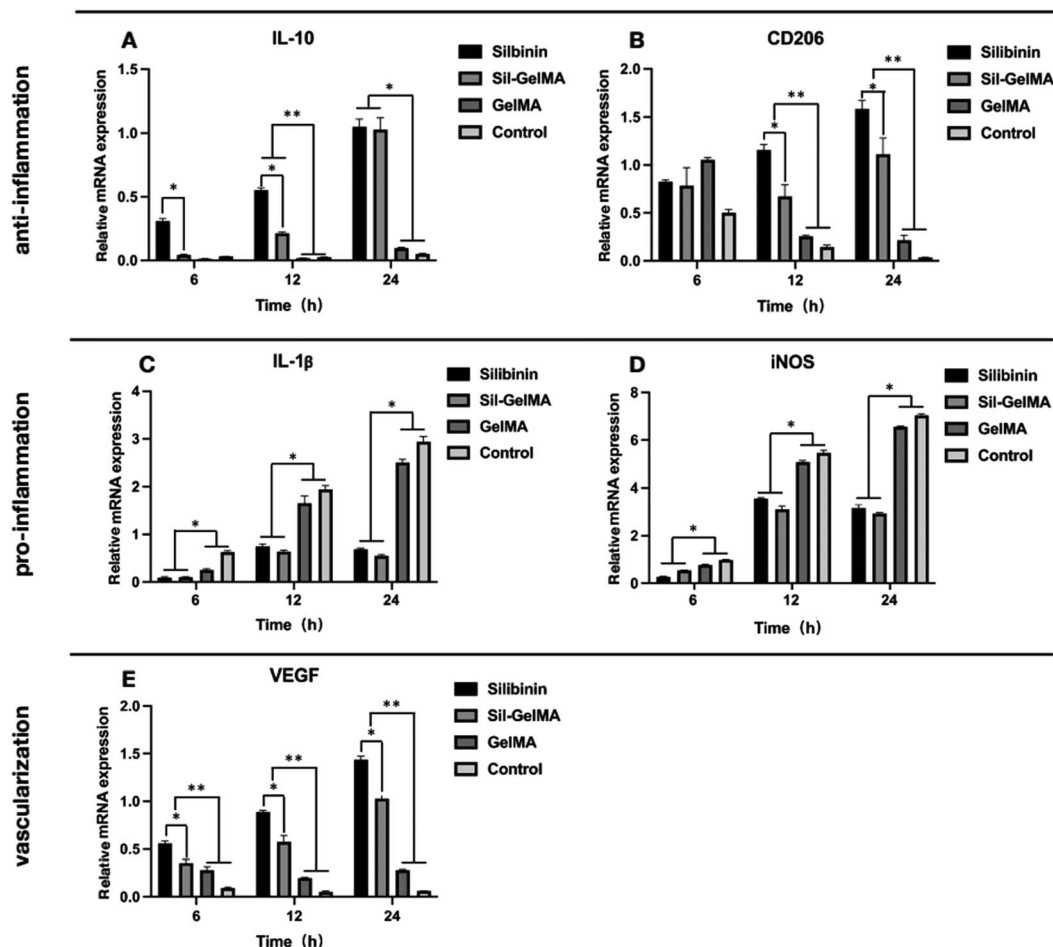


Fig. 11 The mRNA levels of anti-inflammatory, pro-inflammatory and vascularization-related genes were tested after 6, 12, 24 hours culture in different groups. Real-time PCR were used to analyze related gene markers: (A) the mRNA level of IL-10, (B) the mRNA level of CD206, (C) the mRNA level of IL-1 β , (D) the mRNA level of iNOS, (E) the mRNA level of VEGF. "*" and "***" meant significant difference ($p < 0.05$).

Silibinin and Sil-GelMA groups than that of the GelMA and control groups ($p < 0.05$), and there was no difference between the silibinin and Sil-GelMA groups (Fig. 11C and D). IL-1 β is a key mediator of the inflammatory response, which is essential for host-response and resistance to pathogens. It also exacerbates damage during chronic disease and acute tissue injury.⁴⁴ iNOS is one of three isoforms belonging to the family of nitric oxide synthases. Its expression is inducible and is frequently associated with inflammation.⁴⁵ In this study, with the stimulation of LPS, macrophages showed high mRNA expression level of the two pro-inflammation factors in the GelMA and control groups, which meant the macrophages mainly existed as M1-type in normal environment with the stimulation of LPS. With the addition of silibinin, the mRNA expressions of IL-1 β and iNOS decreased, which meant the inhibition of M1-type macrophages in the silibinin and Sil-GelMA groups.

RAW 264.7 cells exhibited both M1-type and M2-type characteristics under LPS stimulation, while M1 was the main polarized type, which was consistent with previous studies.⁴³ When silibinin was released from Sil-GelMA hydrogels, the dynamic balance of the micro-environment was broken, then

macrophages mainly polarized into M2-type with the anti-inflammatory effect, and M1-type with the pro-inflammatory effects was weakened. Studies also proved that macrophage polarization is a dynamic process, once macrophages acquired a functional polarization, it still retains the ability to change in response to new environmental stimulation.⁴⁶

Sil-GelMA hydrogels promote vascularization at an early stage *in vitro*

In multiple tissues, macrophages have been identified as an important regulator of both blood and lymphatic vessel growth, specifically following tissue injury and in pathological inflammatory environment.⁴⁷ To investigate the function of silibinin on vascularization, the expression of VEGF was examined. The results showed that in the silibinin and Sil-GelMA groups, the mRNA level of VEGF was significantly higher than that in the GelMA and control groups at the early stage ($p < 0.05$), and it showed higher mRNA expression level of VEGF in the silibinin group than that in the Sil-GelMA group ($p < 0.05$) (Fig. 11E). In combination with the previous results, the high mRNA level of VEGF was expressed by M2-type macrophages.^{48,49} Meanwhile, it



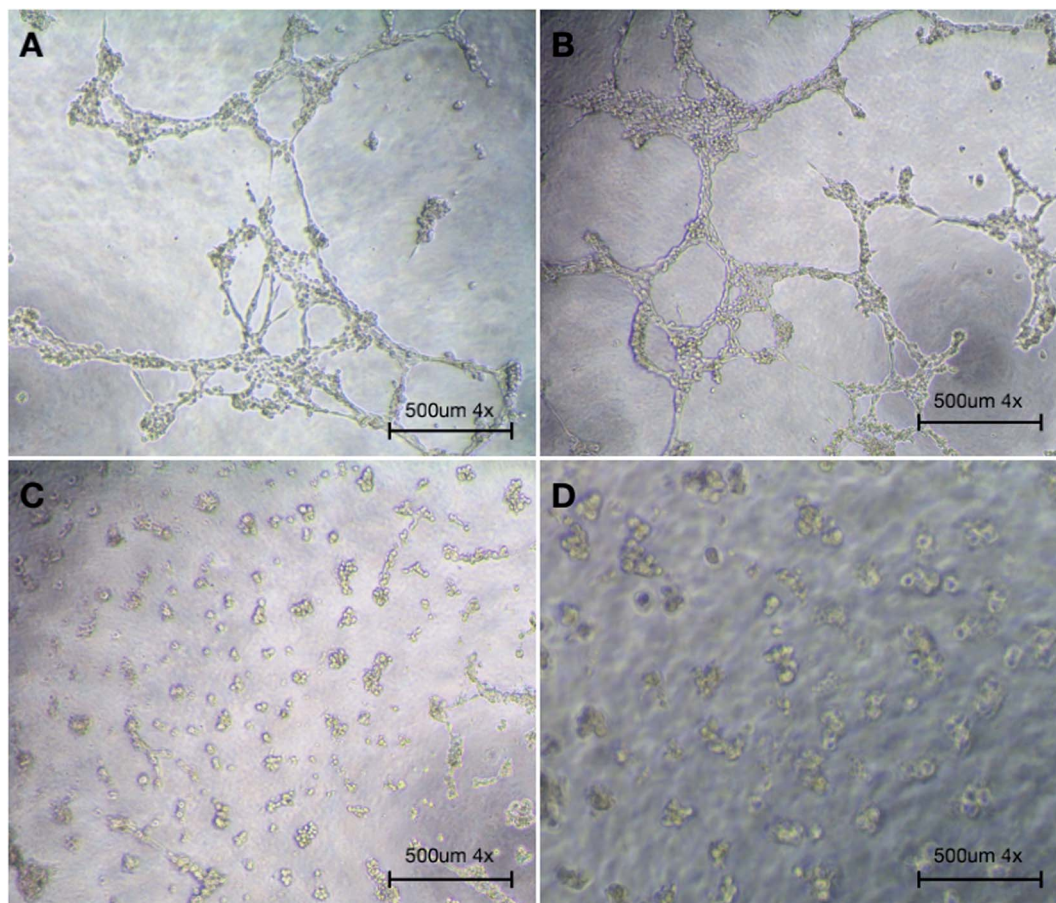


Fig. 12 The result of tube formation assay. HUVECs were cultured in supernatant culture medium of different groups (silibinin, Sil-GelMA, GelMA and the control) for 6 hours. The tube formation phenomenon was observed by optical microscope. (A) The silibinin group, (B) the Sil-GelMA group, (C) the GelMA group, (D) the control group.

could be speculated that silibinin had the effect on promoting vascularization at the gene expression level. To verify its vascularization effect, the tube formation assay was carried out, and the result was showed in Fig. 12. It could be seen that in the silibinin and Sil-GelMA groups, cells connected together and formed tubular structures, which were the early vascular structure (Fig. 12A and B). However, this phenomenon could not be found in the GelMA and control groups (Fig. 12C and D). These results proved that silibinin could promote vascularization *in vitro* at the early stage.

The prevention of dry socket after tooth extraction mainly depends on anti-inflammatory ability and blood clots stabilization. In this study, results suggested that Sil-GelMA hydrogels presented the ability to maintain the space stability in the early 24 hours and could inhibit inflammation and promote vascularization. When inserted into the tooth socket, GelMA hydrogels could occupy the socket and release silibinin, which exhibited the anti-inflammatory and vascularization effect. However this *in vitro* study also has some limitations: the mechanism of how silibinin induces the macrophages to polarize into M2-type and promotes the secretion of VEGF on M2-type macrophages is still unclear, and *in vivo* studies are needed to confirm the results.

Conclusions

In summary, GelMA hydrogels are applied to construct a Sil-GelMA hydrogels sustained-release system, which has good performance on drug sustained release and 3D space occupation. Meanwhile, it is found that silibinin can promote macrophages to polarize into M2-type with increased secretion of anti-inflammatory factors at the early stage, and silibinin also enhances the expression of VEGF and promotes vascularization *in vitro*. Thus, as a biological material, this 3D sustained-release system exhibits a great potential for the prevention of dry socket.

Author contributions

Z. X. and Y. W. conceived and designed the experiments. W. X., Y. S., B. W., and F. X. carried out the experiments. W. X., Y. S., and Y. W. analyzed the data. W. X., and J. W. wrote and revised the manuscript. All authors commented on the manuscript.

Conflicts of interest

There are no conflicts to declare.

Acknowledgements

This work was supported by the National Natural Science Foundation of China (Grant No. 81800934, 81771118). This work was also supported by the Zhejiang Provincial Natural Science Foundation of China (Grant No.: LY22H140002).

Notes and references

- 1 J. Mamoun, *J. Korean Assoc. Oral Maxillofac.*, 2018, **44**, 52–58.
- 2 M. Taberner-Vallverdú, M. Sánchez-Garcés and C. Gay-Escoda, *Med. Oral Patol. Oral Cir. Bucal*, 2017, **22**, e750–e758.
- 3 P. A. Lone, S. W. Ahmed, V. Prasad and B. Ahmed, *J Oral Biol. Craniofac. Res.*, 2018, **8**, 44–47.
- 4 V. Sridhar, G. G. Wali and H. N. Shyla, *J. Oral Maxillofac. Surg.*, 2011, **10**, 101–111.
- 5 L. R. Halpern and T. B. Dodson, *J. Oral Maxillofac. Surg.*, 2007, **65**, 177–185.
- 6 Y. F. Ren and H. S. Malmstrom, *J. Oral Maxillofac. Surg.*, 2007, **65**, 1909–1921.
- 7 H. Cho, H. D. Jung, B. J. Kim, C. H. Kim and Y. S. Jung, *J. Korean Assoc. Oral Maxillofac.*, 2015, **41**, 26–29.
- 8 P. J. Murray and T. A. Wynn, *Nat. Rev. Immunol.*, 2011, **11**, 723–737.
- 9 A. Mantovani, A. Sica, S. Sozzani, P. Allavena, A. Vecchi and M. Locati, *Trends Immunol.*, 2004, **25**, 677–686.
- 10 S. Gordon, *Nat. Rev. Immunol.*, 2003, **3**, 23–35.
- 11 D. M. Mosser, *J. Leukoc. Biol.*, 2003, **73**, 209–212.
- 12 S. Goerdts and C. E. Orfanos, *Immunity*, 1999, **10**, 137–142.
- 13 A. Mantovani, S. Sozzani, M. Locati, P. Allavena and A. Sica, *Trends Immunol.*, 2002, **23**, 549–555.
- 14 D. M. Mosser and J. P. Edwards, *Nat. Rev. Immunol.*, 2008, **8**, 958–969; *Nat. Rev. Immunol.*, 2010, **10**, 460.
- 15 S. C. Funes, M. Rios, J. V. Escobar and A. M. Kalergis, *Immunology*, 2018, **154**, 186–195.
- 16 J. H. Kim, K. Kim, H. M. Jin, I. Song, B. U. Youn, J. Lee and N. Kim, *Mol. Cells*, 2009, **28**, 201–207.
- 17 P. R. S. Davis, Y. Nakanishi, N. C. Kim, T. N. Graf, N. H. Oberlies, M. C. Wani, M. E. Wall, R. Agarwal and D. J. Kroll, *Cancer Res.*, 2005, **65**, 4448–4457.
- 18 N. M. Vargas, Á. G. Morales, M. M. Morales, M. A. U. Soriano, L. O. Delgado, E. M. G. Sandoval, E. B. Madrigal, I. G. Álvarez, E. S. Madrigal and J. A. G. Morales, *Biomedicines*, 2020, **8**, 122.
- 19 J. Chen, D. L. Li, L. N. Xie, Y. R. Ma, P. P. Wu, C. Li, W. F. Liu, K. Zhang, R. P. Zhou, X. T. Xu, X. Zheng and X. Liu, *Phytomedicine*, 2020, **78**, 153309.
- 20 C. K. Youn, S. J. Park, M. Y. Lee, M. J. Cha, O. H. Kim, H. J. You, I. Y. Chang, S. P. Yoon and Y. J. Jeon, *Biomol. Ther.*, 2013, **21**, 258–263.
- 21 C. Ulm, G. D. Strbac, A. Stavropoulos, A. Esfandeyari, T. Dobsak and K. Bertl, *Clin. Exp. Dent. Res.*, 2021, **2021**, 1–6.
- 22 J. Yang, Y. Zhou, F. Wei and Y. Xiao, *Clin. Oral Implants Res.*, 2016, **27**, 1031–1038.
- 23 K. Yue, S. G. Trujillo-de, M. M. Alvarez, A. Tamayol, N. Annabi and A. Khademhosseini, *Biomaterials*, 2015, **73**, 254–271.
- 24 M. Xie, Q. Gao, H. Zhao, J. Nie, Z. Fu, H. Wang, L. Chen, L. Shao, J. Fu, Z. Chen and Y. He, *Small*, 2019, **15**, e1804216.
- 25 X. Zhao, S. Liu, L. Yildirimer, H. Zhao, R. Ding, H. Wang, W. Cui and D. Weitz, *Adv. Funct. Mater.*, 2016, **26**, 2809–2819.
- 26 H. J. Yoon, S. R. Shin, J. M. Cha, S. H. Lee, J. H. Kim, J. T. Do, H. Song and H. Bae, *PLoS One*, 2016, **11**, e0163902.
- 27 J. Wang, L. Xu, Z. Xiang, Y. Ren, X. Zheng, Q. Zhao, Q. Zhou, Y. Zhou, L. Xu and Y. Wang, *Cell Death Dis.*, 2020, **11**, 136.
- 28 M. Fan, S. Chen, Y. Weng, X. Li, Y. Jiang, X. Wang, M. Bie, L. An, M. Zhang, B. Chen, G. Huang, J. Wu, M. Zhu and Q. Shi, *Oncol. Rep.*, 2020, **44**, 91–102.
- 29 F. Ge, M. Yu, C. Yu, J. Lin, W. Weng, K. Cheng and H. Wang, *Colloids Surf., B*, 2017, **150**, 153–158.
- 30 J. W. Nichol, S. T. Koshy, H. Bae, C. M. Hwang, S. Yamanlar and A. Khademhosseini, *Biomaterials*, 2010, **31**, 5536–5544.
- 31 J. A. Benton, C. A. DeForest, V. Vivekanandan and K. S. Anseth, *Tissue Eng.*, 2009, **15**, 3221–3230.
- 32 J. Fibigr, D. Šatinský and P. Solich, *J. Pharm. Biomed. Anal.*, 2017, **134**, 203–213.
- 33 J. Li and D. J. Mooney, *Nat. Rev. Mater.*, 2016, **1**, 16071.
- 34 I. Pepelanova, K. Kruppa, T. Scheper and A. Lavrentieva, *Bioengineering*, 2018, **5**, 55.
- 35 B. A. Nestor, E. Samiei, R. Samanipour, A. Gupta, D. B. A. Van, D. L. D. M. Diaz, Z. Wang, H. R. Nejad, K. Kim and M. Hoorfar, *RSC Adv.*, 2016, **6**, 57409–57416.
- 36 X. Zhang, J. Li, P. Ye, G. Gao, K. Hubbell and X. Cui, *Acta Biomater.*, 2017, **59**, 317–326.
- 37 J. Antunes, V. M. Gaspar, L. Ferreira, M. Monteiro, R. Henrique, C. Jerónimo and J. F. Mano, *Acta Biomater.*, 2019, **94**, 392–409.
- 38 C. D. Mills, K. Kincaid, J. M. Alt, M. J. Heilman and A. M. Hill, *J. Immunol.*, 2000, **164**, 6166–6173.
- 39 S. Gordon and F. O. Martinez, *Immunity*, 2010, **32**, 593–604.
- 40 S. K. Biswas and A. Mantovani, *Nat. Immunol.*, 2010, **11**, 889–896.
- 41 A. Olsson, J. Nakhle, A. Sundstedt, P. Plas, A. L. Bauchet, V. Pierron, L. Bruetsch, A. Deronic, M. Törngren, D. Liberg, F. Schmidlin and T. Leanderson, *J. Immunother. Cancer*, 2015, **3**, 53.
- 42 M. C. Nielsen, G. R. Hvidbjerg, J. Clària, J. Trebicka, H. J. Møller and H. Grønbaek, *Cells*, 2020, **9**, 1175.
- 43 A. J. Pagán and L. Ramakrishnan, *Annu. Rev. Immunol.*, 2018, **36**, 639–665.
- 44 G. Lopez-Castejon and D. Brough, *Cytokine Growth Factor Rev.*, 2011, **22**, 189–195.
- 45 M. Kielbik, I. Szulc-Kielbik and M. Klink, *Int. J. Mol. Sci.*, 2019, **20**, 1751.
- 46 R. D. Stout, C. Jiang, B. Matta, I. Tietzel, S. K. Watkins and J. Suttles, *J. Immunol.*, 2005, **175**, 342–349.
- 47 K. Hadrian, S. Willenborg, F. Bock, C. Cursiefen, S. A. Eming and D. Hos, *Front. Immunol.*, 2021, **12**, 667830.
- 48 A. Khabipov, A. Käding, K. R. Liedtke, E. Freund, L. I. Partecke and S. Bekeschus, *Anticancer Res.*, 2019, **39**, 2871–2882.
- 49 A. Mantovani, S. Sozzani, M. Locati, P. Allavena and A. Sica, *Trends Immunol.*, 2002, **23**, 549–555.

